Molecular Disorder and Structure of Spider Dragline Silk Investigated by Two-Dimensional Solid-State NMR Spectroscopy

Isabelle Marcotte,† Jacco D. van Beek, and Beat H. Meier*

Physical Chemistry, ETH Zurich, CH-8093 Zurich, Switzerland

Received October 24, 2006; Revised Manuscript Received December 18, 2006

ABSTRACT: We have studied the molecular disorder in (^{13}C)Ala- and (^{13}C)Gly-labeled dragline silk from *Nephila edulis* through the distributions of isotropic chemical shifts in one- and two-dimensional ^{13}C−^{13}C NMR spectra obtained under MAS. The alanine residues were found to be present in two distinct major structural environments, in agreement with previous studies, where β-sheets and 3_1-helices were found. The distributions in chemical shift within each residue were found to be uncorrelated, even between spins in the same amino acid residue, and were of similar widths for both the crystalline and noncrystalline parts. Upon long-term mechanical stretching of the silk, the NMR spectra showed no significant changes in conformation nor changes in the degree of disorder but did show increasing structural damage to the silk threads.

Introduction

Spider dragline silk is a high-performance natural fiber with good tensile strength and extensibility.[1,2] It is produced in the abdomen of the spider, in the major ampullate gland, where it is stored in liquid form. After a transitory passage in the spinning duct, it exits from the spinneret as an insoluble solid fiber.[3] Contrary to the highly ordered silk fiber, NMR experiments indicate that the liquid silk in the wide sac of the major ampullate gland does not have a well-defined secondary structure.[4] There is evidence that dragline silk is composed of two proteins, spidroin I and II,[1,5] which contain series of peptide repeats, namely polyalanine motifs (8−10 residues) and glycine-rich sequences with Gly-Gly-X as the most abundant block (X = Gln, Ala, Tyr, Ser, or Leu).[1] Both Gly and Ala-rich domains have a preferred secondary structure and are oriented with the chains mainly parallel to the fiber axis.[6−9] The majority of the alanine residues are found in β-sheets, which include small and well-oriented microcrystalline domains,[2,10−14] while the remaining alanine residues are thought to reside in other conformational environments, which still need to be identified, however.[11] The glycine residues are partly incorporated into the β-sheets and partly into 3_1-helical structures.[8,15]

From such a literature-based model of silk one quintessential aspect is often missing: *disorder*. Disorder in spider dragline silk has been observed by a variety of techniques. Wide-angle X-ray diffraction experiments on silk produced by *Nephila clavipes* have shown that crystals of Ala-rich β-sheets accounted for ∼10% of the material, but that "amorphous oriented" regions represented ∼30% of the fiber.[10] Riekel et al.[16] also observed the presence of disordered crystallites in single threads of *N. clavipes* dragline silk using synchrotron X-ray radiation. Two-dimensional (2D) NMR experiments on *N. edulis* silk have shown order in both local structure and orientation toward the fiber axis, for both the alanine- and glycine-rich domains.[8] Significant distributions in orientational angles, with respect to the fiber axis, and torsion angles were found, but none were wide enough to label the silk disordered in terms of local order ("amorphous") or orientational order with respect to the fiber axis. Furthermore, ^{2}H solid-state NMR experiments on *N. clavipes* silk showed a non-Gaussian distribution in the orientation of the alanine methyl group toward the fiber axis.[6] Transmission electron microscopy (TEM) diffraction data have prompted a non-periodic-lattice description for major-ampullate silk.[17,18] Finally, the disorder is also observed in one-dimensional (1D) ^{13}C NMR spectra obtained under magic-angle spinning (MAS).[11,15] The observed inhomogeneous peak broadening is caused by the variation of isotropic chemical shifts, which are due to slight differences in environment in the fiber.

The goal of this work is to study the disorder in dragline silk by measuring the distributions of isotropic chemical shifts of the alanine and glycine residues, as observed in 1D ^{13}C NMR spectra. The correlation of such distributions in two-dimensional ^{13}C−^{13}C spectra obtained under magic-angle spinning is indicative of the local order in the silk. The same approach is used to study silk under various degrees of mechanical strain.

Materials and Methods

Materials. ^{13}C-labeled dragline silk was collected by forced reeling[19] of *Nephila edulis* spiders at a speed of 20 cm/min. Spiders were kept on a low-diet of *Tenebrio* meal worms with a daily supply of a mixture of amino acids covering the contents of dragline silk, including either fully ^{13}C/^{15}N-labeled alanine or glycine. Labeling started a week before silking. The labeling degree in the silk has not been determined explicitly, but from the ratio of alanine and glycine C_α signals approximate labeling degrees of 17% and 47% were estimated for the alanine- and glycine-labeled samples for Figure 3, assuming 10% and 18% cross labeling,[20] respectively.

Silk Stretching. A cylindrical zirconium oxide spool was used to collect dragline silk from *N. edulis*. The spool was composed of two sections, which could be fitted in a standard 6 mm MAS rotor of the same material, thus limiting magnetic susceptibility effects. A total of 36 mg of silk was wound around the long axis of the spool, which held the two sections together. Stretching of the silk was performed by carefully pulling one section of the spool using a home-built device, and by inserting zirconium oxide spacers of various widths to change the percentage of strain applied to the fibers. Because the silk was spooled on the holders in many overlapping layers, a single degree of stretching cannot be given. Instead the minimum degree of stretching (outer layer) is reported. Note that the silk may well be able to redistribute the differential strain by sliding.

* Corresponding author. E-mail: beme@ethz.ch.
† Current address: Department of Chemistry, Université du Québec à Montréal, C.P. 8888, Succursale Centre-Ville, Montreal, Quebec, Canada H3C 3P8.

10.1021/ma062452n CCC: $37.00
Published on Web 02/17/2007

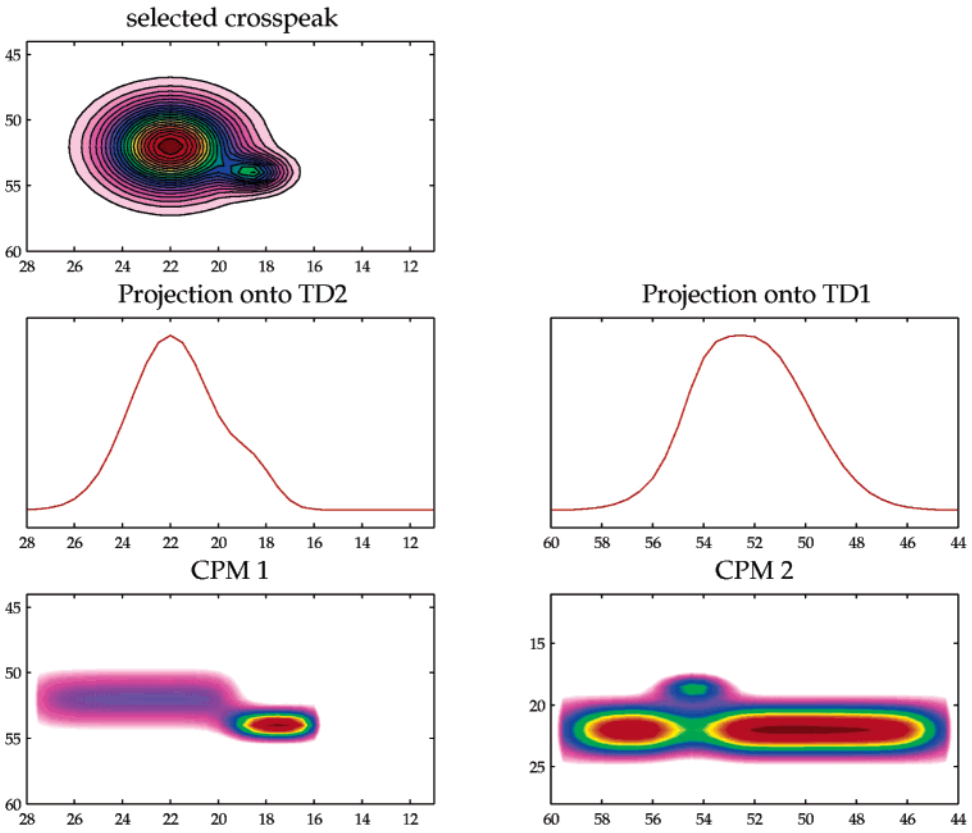

Figure 1. Example of creating a matrix of conditional probabilities (CPM) from a cross-peak in a 2D NMR spectrum for a bimodal Gaussian distribution. The distribution with lowest intensity is narrower and hence amplified in the CPMs. All axes are in ppm.

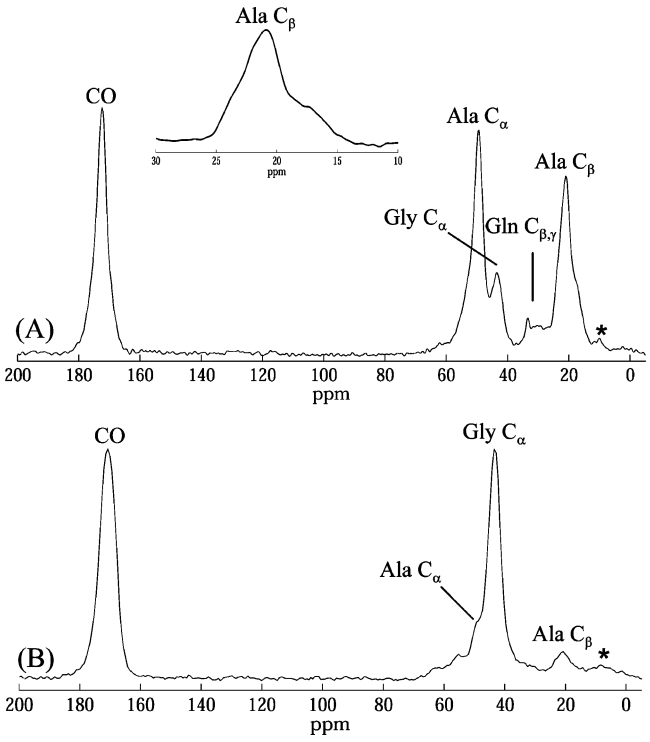

Figure 2. ^{13}C spectra obtained at an MAS frequency of 12.2 kHz for (A) Ala-labeled silk with zoom in on the Ala-C_β peak, and (B) Gly-labeled silk, both from *N. edulis*. Spinning side bands are indicated by asterisks.

Solid-State NMR. All solid-state NMR experiments were performed on a Varian Infinity+ spectrometer operating at a ^1H frequency of 299.17 MHz. The ^{13}C chemical shifts were referenced to external adamantane.[21,22] Two-dimensional $^{13}C-^{13}C$ correlation spectra were obtained using cross-polarization (CP) and proton-driven spin diffusion (PDSD) and magic-angle spinning (MAS) of the sample at a frequency of 12.2 kHz (unstretched silk packed in a 4 mm rotor) or 6.5 kHz (silk on the stretching spool in a 6 mm rotor). Radio-frequency field strength of around 65 kHz were typically used on both channels during cross-polarization, with a contact time of 1−2 ms. A mixing time of 20 ms was employed under rotary-resonance (RR) conditions ($\omega_1 = \omega_r$) for increased spin-diffusion transfer.[23,24] High-power TPPM decoupling[25] (100 kHz) was applied during the acquisition. The relaxation delay was 2 s. A total of 512 data points were acquired in the direct dimension with 170 increments in the indirect dimension (400 for the stretched silk). Gaussian line broadening of 40 Hz was applied to the spectra in both dimensions.

Total through-bond correlation spectroscopy[26] (TOBSY) spectra were obtained at 15.238 kHz MAS using a rotor-synchronized CN_n^ν-type sequence with WURST−inverse−WURST pulses during the mixing period,[27] with 5 $WiW9_{24}^1$ supercycles of 9 WiW elements per 24 rotor cycles. After cross-polarization (2 ms, 90 kHz), 100 kHz TPPM decoupling was applied during the t_1 period which was followed by a z-filter (4 ms). During the $WiW9_{24}^1$ supercycles (7.9 ms) homonuclear proton decoupling under Lee−Goldberg conditions at 143 kHz rf field strength was used, and TPPM decoupling at 100 kHz rf field strength was used during the detection. Gaussian line broadening of 40 Hz was applied to the spectra in both dimensions.

All spectra were processed using the matNMR processing toolbox.[28] A routine to generate conditional probability matrices (CPMs) was incorporated into the matNMR toolbox, which was based on the routines kindly provided by S. Cadars.[29]

Files from the RefDB[30] database were read using a home-written Matlab (www.mathworks.com) script. The chemical-shift referencing in the database was converted from DSS to TMS by substracting 2.00 ppm.[22]

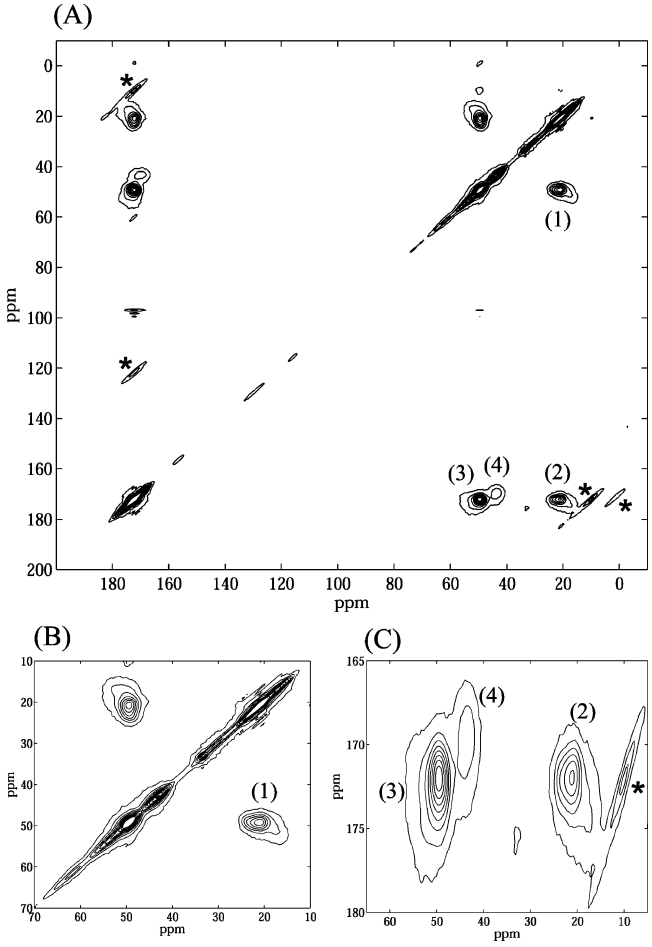

Figure 3. (A) 2D $^{13}C-^{13}C$ proton-driven spin-diffusion correlation spectrum (20 ms) under rotary resonance conditions obtained for Ala-labeled dragline silk produced by *N. edulis* using an MAS frequency of 12.2 kHz. (B) C_α/C_β and (C) $C_\alpha C_\beta$/CO regions. Sidebands are denoted by asterisks, and cross-peaks are labeled as follows: (1) Ala C_β/C_α, (2) Ala Cβ/CO, (3) Ala Cα/CO and (4) Gly C_α/CO.

Disorder and Conditional Probabilities

NMR spectra show disorder through distributions in frequencies. While one-dimensional NMR spectra only show spectral distributions per site, two-dimensional correlation spectra can reveal the correlation of such frequency distributions. The correlation of distributions can be characterized by conditional probabilities $P_B(A)$, which express the probability of the parameter A, given the value for parameter B. Closely related to the probabilities *P* are the conditional (spectral) probability matrices (CPMs) that are obtained by renormalization of the area of a cross-peak in the NMR spectrum. Dividing each row or column of a given area in the 2D spectrum by its sum, leads directly to a matrix with conditional probabilities.[29] The conditional probability matrix shows either the probability that site A resonates at a frequency ω_A given that a site B resonates at ω_B (CPM1), or vice versa (CPM2). If the mapping of A to ω_A were unique then the CPM would directly express the *P*'s. A sample CPM is shown in Figure 1, and more examples can be found in the Supporting Information.

Naturally, CPMs can only highlight information that is also present in a cross-peak itself, but the conditional probability is typically masked by the intensity of a line. CPM plots hence provide a complementary view of the spectrum. From the examples it also follows that CPMs are useful for amplifying small components in a distribution, provided that at least in one dimension the frequency is unique. Also, it allows judging the width of the distribution since this determines the relative intensities in a CPM plot. These features, together with the fact that the conditional probabilities are more closely related to the physical properties than the NMR spectrum, led us to choose the CPM representation for the results to follow.

For proteins, only a few motifs exist for the backbone structure, for example α-helices and β-sheets. These secondary structures lead to easily distinguishable maxima in the CPM plot. In addition, there is a variation in the backbone torsion angles for amino acids that have the same secondary-structure motiv. This variation leads to a distribution of the chemical shifts. It is this additional variation of the chemical shift which we will address in the following.

Results and Discussion

Native Dragline Silk. Figure 2 shows the 1D ^{13}C CP MAS spectra of (A) Ala-labeled and (B) Gly-labeled dragline silk produced by *N. edulis*. The spectra are consistent with a model where the alanine residues are predominantly found in a β-sheet conformation; a shoulder observed on the Ala-C$_\beta$ peak highlighted in the inset of Figure 2A, however, indicates the existence of (an) additional conformational environment(s). This has been observed in NMR spectra previously, for minor-ampullate silk obtained from *N. clavipes*[31] and major-ampullate silk of *N. edulis*.[8,15] The chemical shifts for the glycine residue is rather ambiguous for most commonly observed conformations,[32] hence little information can be obtained from the isotropic chemical shift. The observed resonances in Figure 2 are inhomogeneously broadened due to conformational disorder, i.e., differences in structural environment correlate to differences in the isotropic chemical shift.

We have performed 2D $^{13}C-^{13}C$ proton-driven spin-diffusion (PDSD) experiments to study the correlation of the chemical shifts of spatially neighboring residues. A typical spectrum of alanine-labeled silk, obtained with a mixing time of 20 ms, is presented in Figure 3. The alanine cross-peaks dominate the spectrum, although correlation peaks related to glycine also appear, which indicates that some cross-labeling has taken place. The cross-peaks for the alanine residues do not correspond to a single Gaussian line, as best seen on the $C_\alpha-C_\beta$ cross-peak (Figure 3B and 3C). Furthermore, the heterogeneous line width of the alanine C═O resonance (4.4 ppm fwhh) is considerably broader than, for example, amyloid fibrils.[33] An upper limit to the homogeneous line width can be obtained by looking along the anti-diagonal of the spectrum. For example, the alanine C═O peak on the diagonal in Figure 3a was found to have a 0.85 ppm width (fwhh) along the anti-diagonal, compared to roughly 4.4 ppm along the (asymmetric) diagonal. Note that the line width contains a contribution from the homonuclear *J*-coupling (40 Hz, 0.5 ppm).

Parts A−C of Figure 4 show the CPM analysis applied to the cross-peaks highlighted in Figure 3, parts B and C. The approach reveals the presence of two distinct distributions for alanine residues, with distinct center frequencies for all three sites. The most abundant one, centered at $C_\beta/C_\alpha/C{=}O$ frequencies of approximately 22, 49, and 172 ppm, respectively, indicates the presence of alanine residues in a β-sheet conformation.[34,35] The second distribution is centered at $C_\beta/C_\alpha/C{=}O$ frequencies of approximately 17, 53, and 176 ppm. DOQSY spectra[8] of the same silk have shown the presence of a 3_1-helical structure, suggesting that the second distribution can be assigned to this motiv. Little is known about the chemical shifts in 3_1-helical structures. Previous ^{13}C NMR spectra of $(AGG)_n$ model compounds prepared in a 3_1-helical structure have shown values

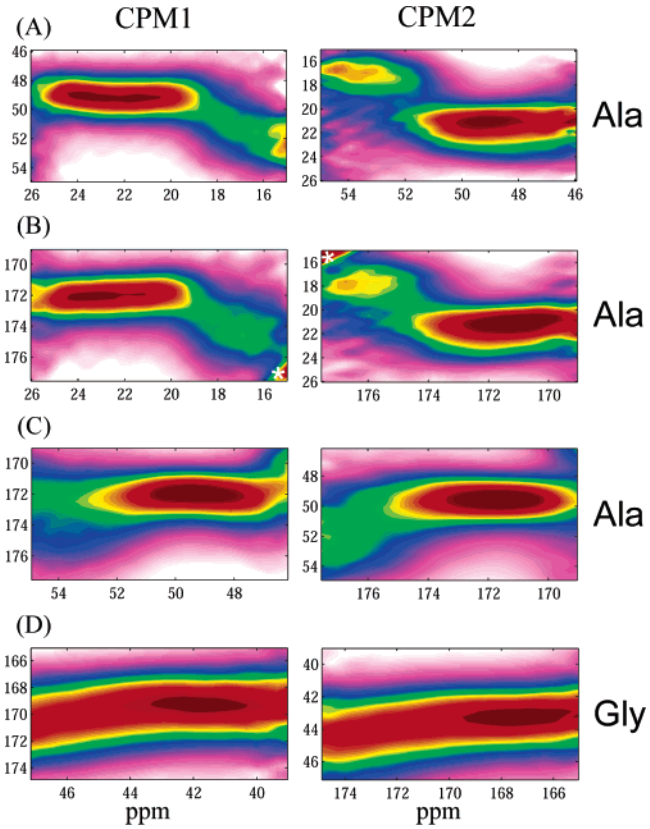

Figure 4. Conditional probability matrices determined from Figure 2 with the (A) Ala C_α/C_β region, (B) Ala CO/C_β region, and (C) Ala CO/C_α region and from (D) the Gly CO/C_α region of the 2D $^{13}C-^{13}C$ correlation spectrum of Gly labeled dragline silk from *N. edulis*. The slant in the CPMs in part D can be attributed to the proximity of Ala C_α/CO centered at 49 /172 ppm. Spinning side bands are indicated by asterisks.

of 17.4, 48.7, and 172.1 ppm,[36] 17.4, 48.9, and 174.6 ppm,[37] and 18.0, 50.0, and 175.6 ppm, respectively.[38] The measured chemical shifts are compatible with those values, although the small size of the databank and errors in determining the centers of the overlapping distributions, estimated at 1−2 ppm, forbid an unambiguous conclusion. Note that the spectra of the model compounds clearly showed disorder to similar degrees as observed in natural silk, despite the control over the preparation.

The CPMs of Gly C_α/CO cross-peak obtained from Gly labeled silk are displayed in Figure 4D. The chemical shift values of glycine cross-peaks often do not allow to discriminate between different conformations, as is known from quantum-chemical calculations that show only minor variations in shift for the most common secondary structures.[32]

The 2D spin-diffusion experiment shows through-space interactions, hence allowing also inter-residue contacts for sufficiently long mixing times. No significant changes in line shape were observed for both diagonal and cross-peaks in spectra taken with mixing times of 200 ms (under rotary-resonance (RR) conditions) or 5 s (without RR, spectra not shown). We have also measured 2D TOBSY[26] spectra where, in contrast, cross-peaks represent only through-bond contacts within one amino acid residue. The resulting CPMs of the alanine cross-peaks are presented in Figure 5. Within experimental accuracy no difference was observed in the shape of the cross-peaks. Similar results were obtained with Gly-labeled silk (not shown).

For a solid protein like silk, the conformation of the backbone, denoted by the torsion angles (ϕ,ψ), is the main parameter

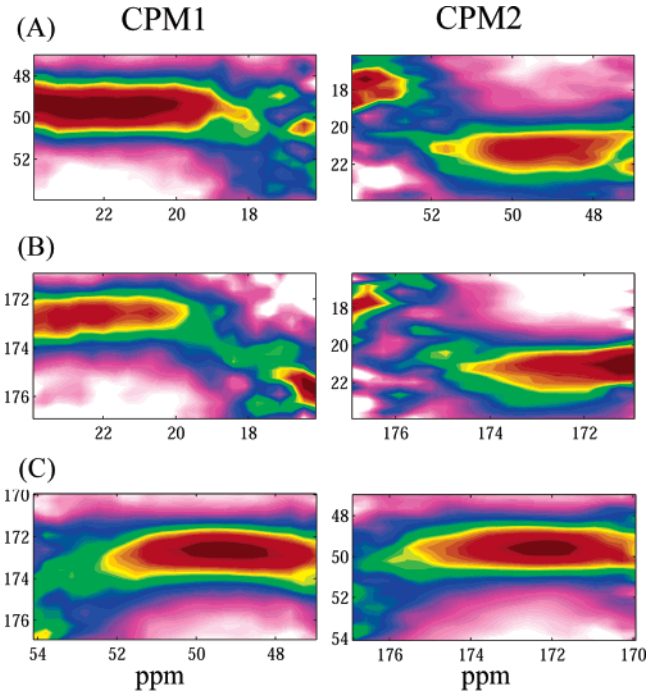

Figure 5. Conditional probability matrices obtained from the TOBSY spectrum (not shown) of Ala-labeled dragline silk produced by *N. edulis*. (A) C_α/C_β, (B) CO/C_β, and (C) CO/C_α regions.

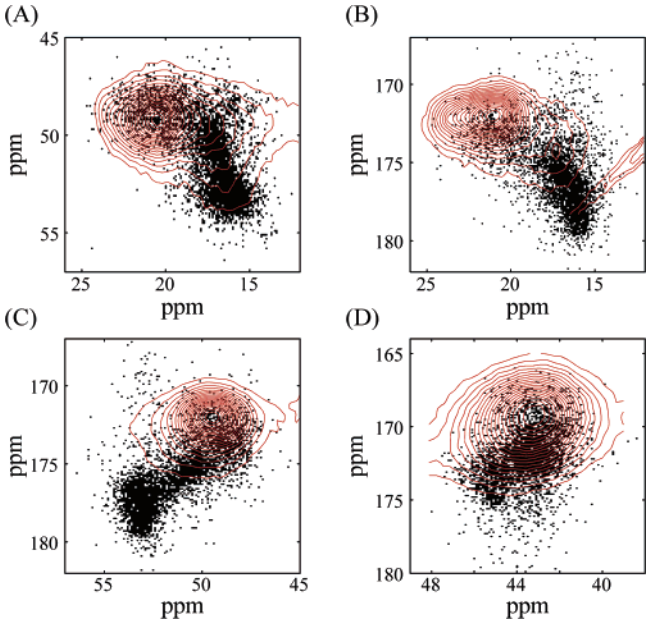

Figure 6. Comparison of the chemical shift range observed in globular proteins (black), as determined from 978 proteins in the RefDB database, and the experimental cross-peaks (red) for the (A) Ala C_α/C_β, (B) Ala CO/C_β, (C) Ala CO/C_α and (D) Gly CO/C_α sites.

contributing to the chemical shift, together with packing effects like hydrogen bonds and steric interactions of side chains. The correlation of secondary structure in proteins and individual chemical shifts is well-known, especially when taken relative to the random-coil shift.[39,40] From a search through 1480 data sets of globular proteins in the RefDB database,[30] 978 were found to contain ^{13}C chemical shifts and plots were made for each amino acid showing the correlations of the CO, C_α, and C_β chemical shifts. The density plots (black) in Figure 6 show the shift correlations for alanine and glycine residues (other amino acids not shown). These plots, while showing the known correlation with structure, reveal no correlation within the ranges

corresponding to the three main structural motifs for proteins in a liquid, i.e., α-helix, β-sheet, and random coil.

The observation of two distinct peaks for the alanine complements previous 2D solid-state NMR spectra and further supports the model proposed from them.[8] While a general correlation of the chemical shift with conformation can be observed from the spectra, an uncorrelated variability of 4−6 ppm width is found in the chemical shifts within these classifications of structure. In silk, this variability is comparable for both the crystalline and noncrystalline parts, and approximately spans the same width as observed for chemical shifts within the β-sheet region in globular proteins (Figure 6). Proteins, in general, have a large variability in amino acid composition, which influences the structure of the protein. Dragline silk of *N. edulis*, however, is thought to have a highly repetitive primary structure with glycine and alanine constituting roughly 70% of the amino acid content. In the absence of accurate chemical-shift calculations for CO and C_β sites, as a function of conformation and packing, it is difficult to quantify the disorder. From an inspection of calculated alanine C_α frequencies,[32] however, deviations in the torsion angles of at least 30° (covering 2σ of a Gaussian distribution) seem required to achieve such widths. This suggests that, regardless of crystalline or noncrystalline parts, on a microscopic scale there is quite a large variability even within a given classification of secondary structure (β-sheet, 3_1-helix, etc.). This is consistent with previous DOQSY measurements where a multimodal distribution of a given width was essential for reproducing the data.[8] This variability includes effects caused by differences in local packing of the molecular chains, the importance of which is hard to estimate. Note that low-temperature NMR spectra have indicated no sharpening of the ^{13}C resonances, thus making it unlikely that motion is responsible for this local disorder.

Disorder plays an important role in semicrystalline polymers[41] and polynucleotide fibers.[42] Contrary to the idea of idealized crystals, irregularities in constitution, configuration or conformation along the polymer chain do not prohibit "crystal" formation, nor diffraction, as long as long-range positional order in one or more dimensions is preserved.[41,43,44] Such a mesomorphic description appears quite natural for silk, given the variations in primary structure and its heterogeneous polymeric nature, and it is based on NMR data, such as those presented here, and diffraction data found in the literature. So far, most diffraction data have, however, been analyzed in terms of a distribution in crystallite sizes. A notable exception is the non-periodic-lattice description by Thiel and Vine[17,18] based on TEM diffraction data. The idea has lost some support after X-ray studies failed to confirm some of the conclusions,[10] but certainly, from the NMR data presented here, such a model would be more appropriate than one with a distribution in crystal sizes but with well-defined conformational order.

Dragline Silk under Strain. Previous NMR findings[8] and the results presented here show that the alanine- and glycine-rich domains, which constitute the vast majority of native dragline silk, are ordered with respect to the fiber and consist of discrete secondary structure elements but with substantial local variations. An open question in this model is what lends silk its elasticity. To study the effect of long-term strain on the local structure and (dis)order we have performed the same 2D NMR analysis on silk which was held at a fixed strain inside the MAS rotor. Here, long-term means that, in contrast to most stress−strain measurements, which are done almost instantaneously, the measurements were started more than 2 h after increasing the strain and the sample was kept at a given strain for at least 1 day. Silk is known to exhibit significant creep and stress relaxation under constant stress and strain, respectively.[45,46] Experiments were first performed on unstrained silk and then on fibers successively stretched by 5%, 10%, 16%, and 21%.

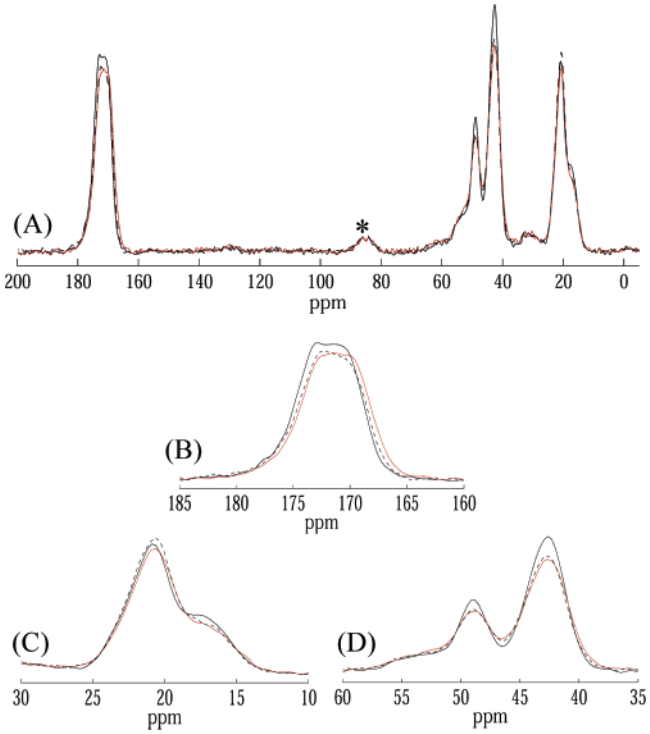

Figure 7. ^{13}C spectrum of Ala/Gly labeled silk from *N. edulis* unstretched (solid black line), stretched by 10% (red line) and 21% (dashed black line) obtained at an MAS frequency of 6.5 kHz. Key: (A) Full spectrum, (B) carbonyl region, and (C) C_β and (D) C_α regions. Spinning side bands are denoted by asterisks.

Figure 7 compares the 1D ^{13}C CP MAS spectra of dragline silk extended by 0%, 10%, and 21%. Only small differences were found between spectra at these various degrees of strain, such as the shoulder in the C_β peak for the alanine residue being slightly less well resolved when tension was applied, suggesting at most minor conformational changes in the crystalline and Gly-rich regions. Note that an exact chemical-shift reference was hard to make for these experiments since the holder had different positions inside the rotor, depending on the degree of strain. This caused small shifts of all lines in the spectrum and was probably due to a susceptibility effect from the Teflon spacers of the MAS rotor, which were cut to accommodate the varying spool length in the course of the experiment. The spectra were superimposed as much as possible by using the chemical shift of glycine C_α in unstrained silk as a reference point, assuming this to be the least sensitive to changes in chemical shift upon stretching.

The CPMs in Figure 8, extracted from 2D PDSD NMR spectra obtained at an MAS frequency of 6.5 kHz, show no changes within experimental error. Note that the signal-to-noise ratio is low due to poorer isotopic labeling. Despite that, one might, for example, expect to observe a narrowing of the chemical-shift distribution in the CPMs upon strain due to an increase of conformational order, which was not observed. Previous 2D spin-diffusion experiments taken from static silk also did not show significant changes in macroscopic and local order upon stretching,[47] suggesting that the stretching does not affect the microscopic ordering of atoms in the silk. Previous NMR[48] and X-ray[10] studies of dragline silk from *N. clavipes*

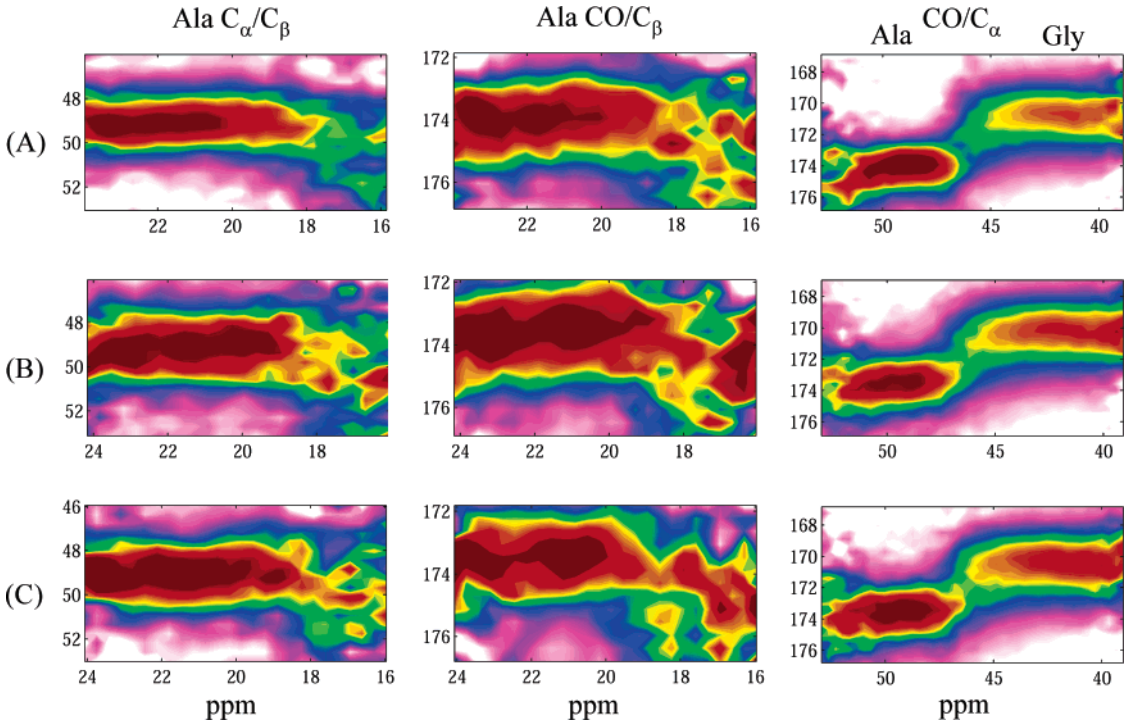

Figure 8. Conditional probability matrices (CPM1) as determined from different regions of the $^{13}C-^{13}C$ correlation spectrum of Ala- and Gly-labeled dragline silk from *N. edulis* obtained at an MAS frequency of 6.5 kHz. Key: (A) 0%, (B) 10%, and (C) 21% stretching.

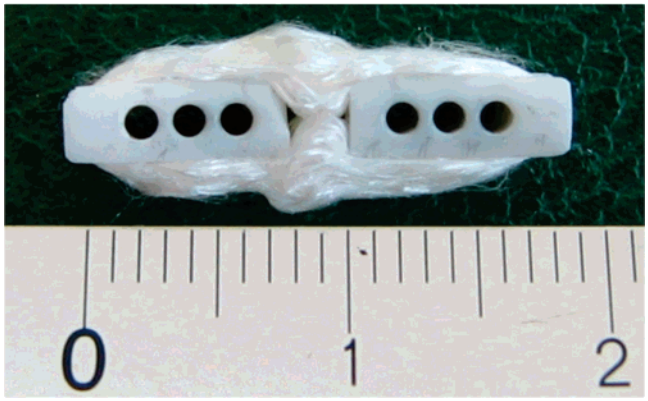

Figure 9. Dragline silk on zirconium oxide spool after removing the insets necessary to stretch the bundle of threads by 21% stretching. The scale is in cm.

report a better alignment of the Ala-rich crystallites in stretched fibers. However, in the light of our results, it appears that such an improved ordering is limited to a macroscopic scale, and that the microscopic order is largely unaffected.

It had been suggested from Raman studies of single dragline silk threads from *N. edulis* that modifications in bond lengths, bond angles and torsion angles occur upon stretching, with an alignment of the molecules along the longitudinal axis of the thread.[49,50] Our experiments are not inherently sensitive to bond lengths and it is unlikely that changes in bond angles could be seen in solid-state NMR spectra of silk, as they are expected to be small. Furthermore, those data on single fibers were measured shortly after the silk was stretched. The bulk samples used here reflect long-term effects of strain, which is likely to be accompanied by significant stress relaxation.[45,46] It may thus be that only a small proportion of alanine and/or glycine residues undergo structural changes under long-term strain. In such a case, the effect would be hidden in the NMR spectra by the broad distribution of chemical shifts.

Finally, the stretching of silk to reach 5% and 10% strain required considerable force, but the material started to yield when trying to achieve 16% stretching. At that point damaged, but not broken, silk threads could be observed. Extension of the silk to 21% was also achieved without much effort, but a greater amount of damaged fibers was seen afterward. The removal of the spacers from the spool revealed a bundle of silk fibers that did not relax back to the original unstrained state (Figure 9). The damage inflicted on the silk by stretching was not localized at a few defective points but distributed evenly. Both 1D and 2D ^{13}C spectra (not shown) of the unstretched silk shown in Figure 9 were superimposable to that of the silk stretched by 21%, indicating irreversible damages on the material.

Conclusion

One- and two-dimensional ^{13}C NMR studies of the dragline silk produced by *N. edulis* show that alanine residues are found in two major discrete local structures, tentatively assigned to β-sheets and 3_1-helices. The chemical shifts of the spins within the same amino acid residue in dragline silk are uncorrelated and the distribution spans the range observed for β-sheets in globular proteins. This implies significant static disorder in both crystalline and noncrystalline domains. Such molecular disorder could be due to variations in conformation or packing within the crystals and would still be consistent with results obtained in diffraction studies.

Long-term mechanical stretching of the dragline silk showed very little influence on the local order in both the alanine-rich and glycine-rich domains, and revealed no changes in conformation. At strains above 10% the silk was increasingly and irreversibly damaged, but no significant changes to the NMR spectra were observed.

Acknowledgment. I.M. wishes to thank the Natural Science and Engineering Research Council (NSERC) of Canada for the award of a postdoctoral fellowship. Matthias Ernst and René

Verel are acknowledged for their precious assistance and advice. We are also very grateful to Andreas Hunkeler for technical assistance and to Fritz Vollrath and Elsa Bomholt Rasmussen for providing the spiders and silk samples.

Supporting Information Available: Figures S1 and S2, showing comparisons of 1D and 2D spectra and conditional probabilities for various simulated line shapes, and text discussing these figures. This material is available free of charge via the Internet at http://pubs.acs.org.

References and Notes

(1) Gosline, J. M.; Guerette, P. A.; Ortlepp, C. S.; Savage, K. N. *J. Exp. Biol.* **1999**, *202*, 3295−3303.
(2) Jelinsky, L. W. *Curr. Opin. Solid State Mater. Sci.* **1998**, *3*, 237−245.
(3) Knight, D. P.; Vollrath, F. *Proc. R. Soc. London, B* **1999**, *266*, 519−523.
(4) Hronska, M.; van Beek, J. D.; Williamson, P. T. F.; Vollrath, F.; Meier, B. H. *Biomacromolecules* **2004**, *5*, 834−839.
(5) Sponner, A.; Schlott, B.; Vollrath, F.; Unger, E.; Grosse, F.; Weisshart, K. *Biochemistry* **2005**, *44*, 4727−4736.
(6) Simmons, A. H.; Michal, C. A.; Jelinsky, L. W. *Science* **1996**, *271*, 81−87.
(7) Shao, Z.; Vollrath, F.; Sirichaisit, J.; Young, R. J. *Polymer* **1999**, *40*, 2493−2500.
(8) van Beek, J. D.; Hess, S.; Vollrath, F.; Meier, B. H. *Proc. Natl. Acad. Sci. U.S.A.* **2002**, *99*, 10266−10271.
(9) Rousseau, M.-E.; Lefèvre, T.; Beaulieu, L.; Asakura, T.; Pézolet, M. *Biomacromolecules* **2004**, *5*, 2247−2257.
(10) Grubb, D. T.; Jelinsky, L. W. *Macromolecules* **1997**, *30*, 2860−2867.
(11) Simmons, A.; Ray, E.; Jelinsky, L. W. *Macromolecules* **1994**, 27, 5235−.
(12) Becker, M. A.; Mahoney, D. V.; Lenhert, P.; Eby, R.; Kaplan, D.; Adams, W.; In *Silk Polymers*, Kaplan, D., Adams, W. W., Farmen, C., Viney, C., Eds..; American Chemical Society: Washington, DC, 1994; pp 185−195.
(13) Riekiel, C.; Vollrath, F. *Int. J. Biol. Macromol.* **1999**, *29*, 203−210.
(14) Sapede, D.; Seydel, T.; Forsyth, V. T.; Koza, M. M.; Schweins, R.; Vollrath, F.; Riekel, C. *Macromolecules* **2005**, *38*, 8447−8453.
(15) Kümmerlen, J.; van Beek, J. D.; Vollrath, F.; Meier, B. H. *Macromolecules* **1996**, *29*, 2920−2928.
(16) Riekel, C.; Bränden, C.; Craig, C.; Ferrero, C.; Heidelbach, F.; Müller, M. *Int. J. Biol. Macromol.* **1999**, *24*, 179−186.
(17) Thiel, B. L.; Kunkel, D. D.; Viney, C. *Biopolymers* **1994**, *34*, 1089−1097.
(18) Thiel, B. L.; Guess, K. B.; Viney, C. *Biopolymers* **1997**, *41*, 703−719.
(19) Work, R. W.; Emerson, P. D. *J. Arachnol.* **1982**, *10*, 1−10.
(20) Hess, S.; van Beek, J. D.; Pannell, L. K. *Anal. Biochem.* **2002**, *311*, 19−26.
(21) Earl, W. L.; Vanderhart, D. L. *J. Magn. Reson.* **1982**, *48*, 35−54.
(22) Morcombe, C. R.; Zilm, K. W. *J. Magn. Reson.* **2003**, *162*, 479−486.
(23) Morcombe, C. R.; Gaponenko, V.; Byrd, R. A.; Zilm, K. W. *J. Am. Chem. Soc.* **2004**, *126*, 7196−7197.
(24) Takegoshi, K.; Nakamura, S.; Terao, T. *Chem. Phys. Lett.* **2001**, *344*, 631−637.
(25) Bennett, A. E.; Rienstra, C. M.; Auger, M.; Lakshmi, K. V.; Griffin, R. G. *J. Chem. Phys.* **1995**, *103*, 6951−6958.
(26) Baldus, M.; Meier, B. H. *J. Magn. Reson.* **1996**, *A121*, 65−69.
(27) Hardy, E. H.; Detken, A.; Meier, B. H. *J. Magn. Reson.* **2003**, *165*, 208−218.
(28) MatNMR is a toolbox for processing NMR/EPR spectra under Matlab and can be freely downloaded at http://matnmr.sourceforge.net.
(29) Cadars, S.; Lesage, A.; Emsley, L. *J. Am. Chem. Soc.* **2005**, *127*, 4466−4476.
(30) Zhang, H.; Neal, S.; Wishart, D. *J. Biomol. NMR* **2003**, *25*, 173−195.
(31) Liivak, O.; Flores, A.; Lewis, R.; Jelinski, L. W. *Macromolecules* **1997**, *30*, 7127−7130.
(32) Havlin, R. H.; Le, J.; Laws, D. D.; deDios, A. C.; Oldfield, E. *J. Am. Chem. Soc.* **1997**, *119*, 11951−11958.
(33) Tycko, R. *Curr. Opin. Chem. Biol.* **2000**, *4*, 500−506.
(34) Saitô, H.; Tabeta, R.; Asakura, T.; Iwanaga, Y.; Shoji, A.; Ozaki, A.; Ando, I. *Macromolecules* **1984**, *17*, 1405−1412.
(35) Saîto, H. *Magn. Reson. Chem.* **1986**, *24*, 835−852.
(36) Saitô, H.; Tabeta, R.; Shoji, A.; Ozaki, T.; Ando, I.; Miyata, T. *Biopolymers* **1984**, *23*, 2279−2297.
(37) Ashida, J.; Ohgo, K.; Komatsu, K.; Kubota, A.; Asakura, T. *J. Biomol. NMR* **2003**, *25*, 91−103.
(38) Nakazawa, Y.; van Beek, J. D.; Asakura, T.; Meier, B. H. Unpublished results.
(39) Spera, S.; Bax, A. *J. Am. Chem. Soc.* **1991**, *113*, 5490−5492.
(40) Wishart, D. S.; Sykes, B. D.; Richards, F. M. *J. Mol. Biol.* **1991**, *222*, 311−333.
(41) Corradini, P.; Auriemma, F.; De Rosa, C. *Acc. Chem. Res.* **2006**, *39*, 314−323.
(42) Stroud, W. J.; Millane, R. P. *Acta Crystallogr.* **1995**, *A51*, 790−800.
(43) De Rosa, C. In *Materials-Chirality*; Topics in Stereochemistry 24, Green, M. M., Nolte, R. J. M., Meijer, E. W., Eds.; Wiley: Hoboken, NJ, 2003.
(44) Auriemma, F.; De Rosa, C.; Corradini, P. *Adv. Polym. Sci.* **2005**, *181*, 1−74.
(45) Smith, C.; Ritchie, J.; Bell, F. I.; McEwen, I. J.; Viney, C. *J. Arachnol.* **2003**, *31*, 421−424.
(46) Morrison, N. A.; Bell, F. I.; Beautrait, A.; Ritchie, J.; Smith, C.; McEwen, I. J.; Viney, C. *Mater. Res. Soc. Symp. Proc.* **2004**, *823*, W8.4.
(47) Kümmerlen, J.; Meier, B. H. Unpublished results.
(48) Elles, P. T.; Michal, C. A. *Biomacromolecules* **2004**, *5*, 661−665.
(49) Sirichaisit, J.; Young, R. J.; Vollrath, F. *Polymer* **2000**, *41*, 1223−1227.
(50) Sirichaisit, J.; Brookes, V. L.; Young, R. J.; Vollrath, F. *Biomacromolecules* **2003**, *4*, 387−394.

MA062452N